Journal of Muscle Research and Cell Motililty

Cross-Bridge Apparent Rate Constants of Human Gallbladder Smooth Muscle

--Manuscript Draft--

Manuscript Number:	JURE356R2
Full Title:	Cross-Bridge Apparent Rate Constants of Human Gallbladder Smooth Muscle
Article Type:	Original Research Paper
Keywords:	gallbladder, active stress, CCK, isometric contraction, acalculous biliary pain, cross-bridge, apparent rate constant, Ca2+, mechanical modelling
Corresponding Author:	Xiaoyu Luo, PhD University of Glasgow Glasgow, UNITED KINGDOM
Corresponding Author Secondary Information:	
Corresponding Author's Institution:	University of Glasgow
Corresponding Author's Secondary Institution:	
First Author:	Wenguang Li, PhD
First Author Secondary Information:	
All Authors:	Wenguang Li, PhD
	Xiaoyu Luo, PhD
	Nicholas A Hill, PhD
	Raymond W Ogden, PhD
	Tianhai Tian, PhD
	Ann Smythe, PhD
	A W Majeed, PhD
	Nigel Bird, PhD
All Authors Secondary Information:	
Manuscript Region of Origin:	
Abstract:	This paper studies human gallbladder (GB) smooth muscle contractions. A two-state cross-bridge model was used to estimate the apparent attachment and detachment rate constants, as well as increased Ca2+ concentration from the peak active stress during the isometric contraction. The active stress was computed from a mechanical model based entirely on non-invasive routine ultrasound scans. In the two-state cross-bridge model, the two apparent rate constants, representing the total attached/detached cross-bridges, respectively, were estimated using active stress prediction for 51 subjects undergoing CCK- provocation test, together with estimates from the four-state cross-bridge model for a swine carotid, bovine tracheal and guinea pig GB smooth muscles. The study suggests that the apparent rate constants should be patient-specific, i.e. patients with a lower stress level are characterized by smaller apparent rate constants. In other words, the diseased GB may need to develop fast cycling cross-bridges to compensate in the emptying process. This is a first step towards more quantitative and non-invasive measures of GB pain, and may provide useful insight in understanding GB motility and developing effective drug treatments.
Response to Reviewers:	Many thanks for reviewing the paper again and for the supportive statement. We have now corrected the typo "mass actin" to be "mass action". We also removed the red colour in the R1 version.

Cross-Bridge Apparent Rate Constants of Human Gallbladder Smooth Muscle

Li W G[1], Luo X Y[1], Hill N A[1], Ogden R W[2], Tian T H[3], Smythe A[4], Majeed A W[4] and Bird N[4]

1 School of Mathematics and Statistics, University of Glasgow, Glasgow, G12 8QW, UK

2. School of Engineering, University of Aberdeen, King's College, Aberdeen, UK
3. School of Mathematical Sciences, Monash University. Melbourne Vic 3800, Australia
4. Academic Surgical Unit, Royal Hallamshire Hospital, Sheffield, S10 2JF, UK

Current date: 06/09/2011

ABSTRACT

This paper studies human gallbladder (GB) smooth muscle contractions. A two-state cross-bridge model was used to estimate the apparent attachment and detachment rate constants, as well as increased Ca^{2+} concentration from the peak active stress during the isometric contraction. The active stress was computed from a mechanical model based entirely on non-invasive routine ultrasound scans. In the two-state cross-bridge model, the two apparent rate constants, representing the total attached/detached cross-bridges, respectively, were estimated using active stress prediction for 51 subjects undergoing CCK-provocation test, together with estimates from the four-state cross-bridge model for a swine carotid, bovine tracheal and guinea pig GB smooth muscles. The study suggests that the apparent rate constants should be patient-specific, i.e. patients with a lower stress level are characterized by smaller apparent rate constants. In other words, the diseased GB may need to develop fast cycling cross-bridges to compensate in the emptying process. This is a first step towards more quantitative and non-invasive measures of GB pain, and may provide useful insight in understanding GB motility and developing effective drug treatments.

Keywords: gallbladder, active stress, CCK, isometric contraction, acalculous biliary pain, cross-bridge, apparent rate constant, Ca^{2+}

1 Introduction

The gallbladder (GB) is an organ that stores bile, a liquid which helps with digestion. During fasting, the sphincter of Oddi is closed, and the pressure difference between the liver and GB drives bile into the GB. This is called the refilling phase. The GB displays adaptive relaxation so it tolerates chamber volume during refilling without an increase in pressure. After a meal, a hormone Cholecystokinin (CCK), initiates GB contraction and sphincter of Oddi relaxation simultaneously, causing the emptying and ejecting bile into the duodenum.

Acalculous biliary pain is biliary colic without gallstones, usually occurring in young women. As drug therapy seems to have no proven benefit, the usual treatment for acalculous biliary pain is laparoscopic cholecystectomy. Causes of acalculous biliary pain may include undetectable tiny stones, poor gallbladder (GB) emptying, hyper-sensitive biliary tract, sphincter of Oddi dysfunction, etc. This may be diagnosed using ultrasonographic examination and cholescintigraphy with cholecystokinin (CCK) infusion to measure GB emptying property (Cozzolino et al. 1963). Such a CCK provocation test is a common means to identify acalculous biliary pain clinically, and also sometimes used to select patients for cholecystectomy (Williamson 1988). Unfortunately, only about 50% of patients' pain symptoms disappear after cholecystectomy (Smythe et al. 1998; Smythe et al. 2004), suggesting that cholecystectomy did not eliminate the source of pain. In order to improve the diagnostic technique, we need to understand better the causes of acalculous biliary pain. This is the purpose of our study.

A positive correlation between GB pain and peak stress in the GB wall was identified in our previous paper (Li et al. 2008) and further work was carried out to evaluate both the passive and active stresses from the measured volume data with ultrasound for individual subjects (Li et al. 2011). This showed that active stress plays a very important role in GB pain and it is essentially patient-dependent.

At the micro-structure level, active stress of smooth muscle can be modelled effectively using the three-element approach, involving a Ca^{2+} driven cross-bridge contracting element, two passive springs respectively in series and in parallel (Zulliger et al. 2004; Stålhand et al. 2008; Kroon 2009). Such an approach leads to new constitutive formulations of smooth muscle to form a framework for soft tissue modelling.

The idea of this paper is to link the cross-bridge models and stress in human GB smooth muscle, and to apply it to a dataset of 51 GB subjects. For this purpose, we briefly introduce current research on cross-bridges in GB smooth muscle cells. At a high CCK

(CCK-8) concentration of 10^{-6}~10^{-4}mM/L for human GB intact smooth muscle cells or 10^{-4}~10^{-2}mM/L for muscle strips (Yu et al. 1994), it is believed that the intracellular free calcium (Ca^{2+}) above a certain concentration triggers a series of events, which leads to force generation in the GB smooth muscle (Yu et al. 1998). It has been shown that the contraction induced by CCK requires a certain level of extracellular Ca^{2+} concentration, and utilizes increased intracellular Ca^{2+} (Brotschi et al. 1989; Shaffer et al. 1992). In other words, GB smooth muscle contracts via the high CCK dose pathway.

It was demonstrated that Ca^{2+} calmodulin-dependent phosphorylation of the 20,000-dalton myosin light chain by myosin light chain kinase (MLCK) and dephosphorylation by myosin light chain phosphatase (MLCP) are responsible for contraction of arterial, airway, vascular and uterine smooth muscle (Hai and Murphy 1988a). It is postulated that a latch-bridge is formed by dephosphorylation of an attached phosphorylation and cross-bridge and that latch-bridge formation and detachment are driven by mass action. The structure of four-state model is shown in Fig.1(a) (Hai and Murphy 1988a). Two conditions are set in order to get a unique set of rate constants. Firstly, the rate constants of phosphorylation of MLCK and dephosphorylation of MLCP are assumed to be equal, i.e. K_1=K_6 and K_2=K_5. Secondly, the attachment-to-detachment ratio is chosen as 4:1, i.e. K_3/K_4=4(Hai and Murphy 1988a). This model is myosin regulation-based.

The myosin regulatory four-state cross-bridge model was later extended to deal with the active stress in both isometric and isotonic processes with a variable rate constant $K_1 (= K_6)$ (Hai and Murphy 1989; Yu et al. 1997; Yang et al. 2003a; Yang et al. 2003b; Zulliger et al. 2004; Bursztyn et al. 2007; Kroon 2009; Murtada et al. 2010; Mbikou et al. 2011). However, all these models require several tissue parameters as well as the [Ca^{2+}] profile with time. Unfortunately, to the best knowledge of the authors, no such data are available for human GB smooth muscles. Therefore the extended four-state model cannot be readily used in our problem.

To simplify the model and reduce the number of required experimental parameters, Hai & Murphy (1988b) converted the four-state cross-bridge model into a two-state cross-bridge model (Huxley 1957) by lumping together dephosphorylated and phosphorylated cross-bridges (Hai and Murphy 1988b; Yu et al. 1997), see Fig. 1(b). Although this model is simplified with only two apparent rate constants, these parameters can usefully indicate the averaged rates of total cross-bridge attachment/detachment, and are thus of clear physical

significance. This is the model we use for the most part of the work. However, the four-state model is also used to estimate range of parameters using available animal data.

Unlike most of the existing studies, which make use of measured parameters in strips of smooth muscles to estimate the active stress, an inverse process is employed in this paper. Rather than using experimental data to determine the coefficients, we use the active stress estimated from a mechanical model based on patient-specific ultrasound scan data (Li et al. 2011) to determine the parameters of GB smooth muscle, such as the cross-bridge rate constants, and Ca^{2+} levels, for 51 human subjects. The major questions are whether these parameters are patient-dependent, and if they are correlated to GB pain. The advantage of this investigation is that the ultrasound scan data are part of routine clinical diagnosis, so we can gain insight of the micro-structure of the GB smooth muscles without expensive, invasive testing. Any insights into the micro-structure malfunction will be useful not only for cholecystectomy selection, but also for potential drug treatment. This work represents the first attempt to relate the CCK-induced GB pain to smooth muscle cell cross-bridge kinetics.

3 Methods

3.1 Two-State Cross-bridge Model

The structure of the equivalent two-state cross-bridge model and the relation used are shown in Fig.1(b). Square brackets [.] are used to denote the concentration of species. Following Zhang et al. (2006), we define $r(t^*)$ as the fraction of attached cross-bridge, which is proportional to [$A_{active}\mathfrak{M}$], at time t^*. The fraction of detached cross-bridges is $1-r(t^*)$, and the exchange between the attached and detached cross-bridge (i.e. between $A_{active}\mathfrak{M}$ and $A_{active}+\mathfrak{M}$) is governed by the equation

$$\frac{dr(t^*)}{dt^*}=\left[1-r(t^*)\right]f_{app}-r(t^*)g_{app} \qquad (1)$$

where f_{app} and g_{app} are the apparent rate constants for attachment and detachment, respectively (Hai and Murphy 1988b). These are related to the original four-state-model parameters, K_1, to K_7 by

$$\begin{cases} f_{app}=\dfrac{K_1K_3\left(K_4K_6+K_4K_7+K_5K_7\right)}{\left(K_1+K_2\right)\left(K_4K_6+K_4K_7+K_5K_7\right)+K_3K_5K_7} \\ g_{app}=\dfrac{K_4K_6+K_4K_7+K_5K_7}{K_5+K_6+K_7} \end{cases}. \qquad (2)$$

Eq. (1) represents chemical reactions in the cross-bridges of smooth muscle cells. We determine the time scale of these reactions from an in vivo experiment for a number of patients at the Royal Hallamshire Hospital, Sheffield. In the experiment, a specific amount of CCK was injected into the patient intravenously and the internal pressure inside the GB was monitored with a miniature pressure transducer simultaneously. A typical recording of GB pressure response under a CCK stimulant is shown in Fig. 2. It shows that by about 14 seconds the GB pressure reaches a higher steady level. This suggests the time scale of the reaction described by Eq. (1) is around 14 sec for GB smooth muscle.

In the CCK provocation test, patients with acalculous biliary pain were given an intravenous infusion of saline (control) followed by a continuously intravenous infusion of CCK (0.05 μg/kg body weight) for 10min to diagnose attacks of biliary-type pain. After 10 minutes, pressure reaches its peak inside the GB wall and the emptying began. Clearly, the CCK infusion time scale (~10min) is much longer than the CCK induced reaction time scale (~14 sec) for cross-bridges. Therefore we can reasonably assume that the chemical reaction in (1) reaches the steady state at each incremental level of CCK, i.e.

$$(1-r)\, f_{app} - r g_{app} = 0 \ . \tag{3}$$

Solving (3) for r gives

$$r = \frac{f_{app}}{f_{app} + g_{app}} = \frac{1}{1 + g_{app} / f_{app}} \ . \tag{4}$$

Note that although r, f_{app} and g_{app} are independent of the reaction time t^*, they are CCK dose-dependent, hence are dependent on the much-slower CCK infusion time t.

To calculate the mechanical stresses at each CCK dose, we assume that the attached cross-bridges, both the phosphorylated and dephosphorylated, behave as linear springs exerting forces proportional to their displacement x from the zero-force equilibrium position. From the Huxley's two-state linear stress model we know that r and the stress σ^a in the steady state are implicitly related by:

$$\sigma^a = \int_{-\infty}^{\infty} kxn(x)dx, \quad r = \int_{-\infty}^{\infty} n(x)dx, \tag{5}$$

where k is the spring constant, and $n(x)$ is the distribution of the fraction of cross-bridges within displacement x. The cross-bridges detach when the displacement is either negative or greater than a critical value (defined as x=1, x being the normalized displacement). If we assume that in the isometric state, $n(x) = n_0$, is independent of x, i.e.

$$n(x)=\begin{cases} n_0, & 0 \le x \le 1 \\ 0, & \text{otherwise} \end{cases}, \tag{6}$$

Then equation (5) leads to

$$\sigma^a = \frac{kn_0}{2}, \quad r=n_0 \ . \tag{7}$$

During the CCK infusion period, the active stress is dose-dependent and increases with the infusion time scale *t*. Accordingly, r , f_{app} and g_{app} are functions of *t*. From Eq. (7), the fraction of attached cross-bridges $r(t)$ is proportional to the active stress, and thus

$$r(t)=\alpha\sigma^a(t),\ \alpha=\frac{r_{max}}{\sigma^a_{max}} \ . \tag{8}$$

Here the maximum active stress, σ^a_{max} is a constant for any individual GB smooth muscle, and the peak fraction of attached cross-bridges, r_{max}, is also a constant. It is known that for cardiac muscle; r_{max} =0.3-0.53 (Robertson et al. 1981; Solaro and Rarick 1998), but for smooth muscle, r_{max} =0.5-0.78 due to the latch-bridge effect (Kamm and Stull 1985a; Hai and Murphy 1988a; Hai and Murphy 1988b; Ratz et al. 1989; Hai 1991).

Substituting Eq. (8) into Eq. (3), we relate the cross-bridge kinetics to $\sigma^a(t)$ by

$$\left[1-\alpha\sigma^a(t)\right] f_{app}(t)-\alpha\sigma^a(t)\,g_{app}(t)=0 \ . \tag{9}$$

Equation (9) can also be written as

$$f_{app}(t)=\alpha\left[\frac{\sigma^a(t)\,g_{app}(t)}{1-\alpha\sigma^a(t)}\right] . \tag{10}$$

3.2. Estimation of the active stress due to CCK

$\sigma^a(t)$ is the peak active stress in the GB during the isometric contraction (CCK infusion period), see Fig. 3(a). This is estimated from a mechanical model (Li et al. 2011). For completeness, we now summarize the key points of the stress estimation.

In the isometric phase, the active stress is determined by the transmural pressure and the geometry of the GB:

$$\sigma^a(t)=\left[p(t)-p_e\right]\max\{F_\theta F_n, F_\varphi/F_n\} \ , \tag{11}$$

where $\max\{F_\theta F_n, F_\varphi/F_n\}$ means pick up the maximum from $F_\theta F_n$ and F_φ/F_n, the F_θ, F_φ, and F_n are geometrical functions given by:

$$\begin{cases} F_\theta\left(h_{GB},D_3,k_1,k_2,\varphi\right)=\dfrac{D_3k_1k_2}{4h_{GB}}\left(1-\dfrac{k_1^2-k_2^2}{k_1^2k_2^2}cos\,2\varphi\right) \\ F_\varphi\left(h_{GB},D_3,k_1,k_2,\theta,\varphi\right)=\dfrac{D_3}{4k_1k_2h_{GB}}\left[k_1^2k_2^2+\left(k_1^2+k_2^2-2k_1^2k_2^2\right)sin^2\,\theta+\left(k_1^2-k_2^2\right)cos^2\,\theta cos\,2\varphi\right] \\ F_n\left(k_1,k_2,\theta,\varphi\right)=\dfrac{\sqrt{k_1^2\,cos^2\,\theta cos^2\,\varphi+k_2^2\,cos^2\,\theta sin^2\,\varphi+sin^2\,\theta}}{\sqrt{k_1^2\,sin^2\,\varphi+k_2^2\,cos^2\,\varphi}}, \end{cases} \quad (12)$$

where D_1, D_2, D_3 are the three principal diameters of the ellipsoid fitting the GB shape, and h_{GB} is the GB wall thickness. Note that $k_1=D_1/D_3$ and $k_2=D_2/D_3$ are constant and are estimated from the ultrasound scans of GB of patients in the isometric period. p_e =11mmHg is the refilling pressure (Li et al. 2011). θ and φ are the angular coordinates of a spherical coordinate system on the ellipsoid GB wall (Fig. 3b) (Li et al. 2011). Note by taking the maximum value of the geometrical functions we ensure that σ^a takes the maximum in-plane stress component at any particular location of the ellipsoid.

The peak active stress occurs at the end of the isometric contraction:

$$\sigma_{max}^a=\left(p_{max}-p_e\right)\max\{F_\theta F_n,F_\varphi/F_n\}\ . \quad (13)$$

where p_{max} is the GB pressure at the end of CCK induced isometric contractions.

In our study, the isometric contraction was induced by infusion of CCK to patients over the period of 10 minutes (Smythe et al. 1998), so that it is reasonable to assume that the isometric contraction is a quasi-steady process during which time the concentration of CCK is steadily increased. We assume that during this quasi-steady isometric contraction, the GB shape remains ellipsoidal, so the shape functions F_θ, F_n, F_φ are independent of time, while the pressure in the GB obeys (Meiss 1975)

$$p\left(t\right)=p_e e^{\lambda t},\ \ \lambda=\ln\left(\frac{p_{max}}{p_e}\right)\Big/t_i\ , \quad (14)$$

where t_i is the GB isometric contraction time during the course of CCK injection (10 min), and λ is a constant. Then $\sigma^a\left(t\right)/\sigma_{\max}^a$ can be expressed as

$$\sigma^a\left(t\right)\Big/\sigma_{\max}^a=\left(e^{\lambda t}-1\right)\Big/\left(e^{\lambda t_i}-1\right)\ , \quad (15)$$

From Eq. (10) and (15), we have

$$f_{app}(t)=\frac{r_{max}\left(e^{\lambda t}-1\right)g_{app}(t)}{\left(e^{\lambda t_i}-1\right)-r_{max}\left(e^{\lambda t}-1\right)}\ . \tag{16}$$

Note that the rate constants in Eq. (16) appear to be the function of time. This is because they are thought to be functions of $[Ca^{2+}]$ which increase as CCK is infused. This time dependence is much slower than the transient change in Eq. (1). Eq. (16) also shows that although f_{app} is dependent on the value of λ, the final value of $f_{app}^{max}\left(\text{when } t=t_i\right)$ is proportional to g_{app} only, for a given value of r_{max}. This makes sense, since a faster cycling process requires both higher rates of constants of cross-bridge attachments and detachments.

3.3 Estimation of g_{app} for human GB

It remains to determine the apparent rate constant g_{app}. It has been found that the g_{app} is nearly independent of $[Ca^{2+}]$ and approximately unchanged in the cycling of cross-bridges (Brenner 1988). Therefore we can assume that g_{app} is independent of time. Unfortunately, there are no direct experiments for human GB to help us to find the range of values of g_{app}, so we need to estimate it from the limited data available for smooth muscles of guinea pigs. Our estimation is based on using the four-state cross-bridge model for swine artery, bovine tracheal and guinea pig GB smooth muscles, where the active stress and Mp and AMp concentrations were measured. This helps us to identify the relevant constants, K_1-K_7 for the guinea pig's smooth muscle contractions.

In order to determine the rate constants K_1 through K_7, when there is an unlimited supply of Ca^{2+}, and hence the maximum values $f_{app}^{\max}$ and $g_{app}^{\max}$, we solved the four-state cross-bridge model for smooth muscle proposed by (Hai and Murphy 1988a) (Fig.1a)

$$\begin{cases}\dfrac{d[\mathrm{M}]}{dt^*}=-K_1[\mathrm{M}]+K_2[\mathrm{Mp}]+K_7[\mathrm{AM}]\\ \dfrac{d[\mathrm{Mp}]}{dt^*}=K_4[\mathrm{AMp}]+K_1[\mathrm{M}]-(K_2+K_3)[\mathrm{Mp}]\\ \dfrac{d[\mathrm{AMp}]}{dt^*}=K_3[\mathrm{Mp}]+K_6[\mathrm{AM}]-(K_4+K_5)[\mathrm{AMp}]\\ \dfrac{d[\mathrm{AM}]}{dt^*}=K_5[\mathrm{AMp}]-(K_7+K_6)[\mathrm{AM}],\end{cases} \tag{17}$$

numerically using the 4th-order Runge-Kutta method, with the initial condition $[\mathrm{M}]=1$, $[\mathrm{Mp}]=[\mathrm{AMp}]=[\mathrm{AM}]=0$. (Note that here we use the fast reaction time scale, t^*.)

The results are used to match the experimental data obtained for swine carotid artery smooth muscle (Singer and Murphy 1987), tracheal smooth muscle (Kamm and Stull 1985b), and guinea pig GB smooth muscle (Washabau et al. 1994) by choosing suitable set of rate constants K_1 through K_7, see Fig. 4. The rate constants K_1 through K_7 for the swine carotid artery smooth muscle and tracheal smooth muscle are found to be the same as given by Hai and Murphy (1988a). The rate constants K_1 through K_7 for the guinea pig GB smooth muscle are determined here which give the best experimental fit for the time dependent active stress and the concentration [Mp]+[AMp], see Fig. 4.

All the estimated rates of constants are listed in Table 1. Note that $r_{\max} = (1 + g_{app}^{\max} / f_{app}^{\max})^{-1}$ is about 0.77 for both the swine carotid artery and bovine carotid smooth muscles, this agrees with experimental observations (Kamm and Stull 1985a; Hai and Murphy 1988a; Hai and Murphy 1988b; Ratz et al. 1989; Hai 1991). Choosing the same value $r_{\max}$ =0.77 for the guinea pigs' GB smooth muscle, we obtain $f_{app}^{\max} = 0.0553$, which is about 3.6 times $g_{app}^{\max}$, consistent with the experimental observation on rabbit psoas fibres (Brenner 1988). Table 1 also suggests that the apparent rate constant g_{app} should be around $0.015s^{-1}$ for the GB smooth muscle. It is interesting to see that the rate constants are highly dependent on the smooth muscle groups selected. The apparent rate constants $f_{app}^{\max}$ and $g_{app}^{\max}$ of guinea pig GB smooth muscle are considerably smaller than those of swine carotid artery and tracheal smooth muscle. This is presumably because the strength and frequency of the contraction required in the GB is much lower than that of carotid artery and trachea. Given that GB smooth muscles function the same way in human, it is reasonable to assume that human GB smooth muscle has a comparable g_{app}^{max} value to that of guinea pigs'.

However, although for each individual subject, g_{app}^{max} is a constant, it is not clear if it is constant across a range of patients in pathological cases. In other words, patients constantly require a higher level of active stress may develop faster cycling cross-bridges. This hypothesis is supported by the observation in Table 1, that organs of different functions develop different values of the rate constants. We thus explore the possibility of g_{app}^{max} being proportional to the peak active stress of each individual GB, i.e.

$$g_{app}^{\max} = \beta \sigma_{\max}^{a}, \quad . \tag{18}$$

where β is a constant chosen to be $g_{app}^{mean} / \sigma_{mean}^{a}$, σ_{mean}^{a} =59mmHg is the mean peak active stress level based on the 51 sample of GBs, and g_{app}^{mean} is the mean apparent detachment rate constant for human GB, chosen to be 0.015s^{-1} (Table 1), implying that $\beta = 2.54\ (\text{mmHg}\cdot\text{s})^{-1}$.

3.4 Active stress and the Ca^{2+} level

The CCK-induced GB contraction utilizes Ca^{2+} from the intracellular stores (Lee et al. 1989; Renzetti et al. 1990; Shaffer et al. 1992). Although the relationship between the active stress and $[Ca^{2+}]$ is time-dependent and implicit through the constants K_1 and K_7 of the cross-bridge model (Hai and Murphy 1988a), if we only consider the steady state as discussed in 3.1, then the steady active stress should be proportional to the total increase of $[Ca^{2+}]$ supplied, i.e.

$$\Delta\left[Ca^{2+}\right] = \gamma\sigma^{a}(t) \ . \tag{19}$$

where γ is a constant. In fact, this relationship between the steady active stress and $\Delta\left[Ca^{2+}\right]$ was reported in experiments (Ishizuka et al. 1993) The simplest approach is to choose γ to be $\Delta\left[Ca^{2+}\right]^{mean} / \sigma_{mean}^{a}$, where $\Delta\left[Ca^{2+}\right]^{mean}$ and σ_{mean}^{a} are the averaged quantities of a normal human GB. σ_{mean}^{a} can be calculated from the average value of the active stress of the 51 GB samples (σ_{mean}^{a} =59 mmHg), but $\Delta\left[Ca^{2+}\right]^{mean}$ again needs to be estimated from the experimental data for guinea pigs.

For adult guinea pig GB, the mean intracellular free Ca^{2+} level in normal GB smooth muscle is about 82.5 nM/L (Shen et al. 2007), and the mean intracellular free Ca^{2+} level in healthy guinea pig heart muscle is about 151 nM/L (Thompson et al. 2000). Therefore the ratio of the mean free Ca^{2+} of smooth and heart muscles for guinea pig GB is about 0.546. For human myocardium, the resting intracellular free Ca^{2+} level is around 250nM/L (Gwathmey and Hajjar 1990; Beuckelmann et al. 1992). In the absence of experimental data on human gallbladder muscle, it is not unreasonable to assume that the ratios would be similar which would produce a free $\left[Ca^{2+}\right]^{mean}$ in human GB smooth muscles around 250*0.546=136.6nM/L. We also know that the peak value of Ca^{2+} for the guinea pig GB smooth muscles is normally 17% higher than the resting level under the CCK-8S stimulus of 50μM/L (Si et al. 2009). Applying the same percentage to human GB smooth muscles, we have $\Delta\left[Ca^{2+}\right]^{mean}$ =136.6*0.17=23.2 nM/L.

4 Results

The peak apparent rate constant $f_{app}^{\max}$ for the 51 human GBs after the end of the CCK infusion are calculated using Eq. (16) and (18), is shown in Table 2, together with the bile ejection fraction (EF) at 30min of emptying, the peak active stress, λ, f_{app}, g_{app} and increased $\Delta\left[Ca^{2+}\right]$. The results show that if we choose constant $g_{app}^{\max}$ ($0.015s^{-1}$), then f_{app} is insensitive to the change in the active stress ($f_{app}^{\max} \approx 0.05s^{-1}$). However, if we let g_{app} vary according to Eq. (18), then the peak $f_{app}^{\max}$ changes in the range of ($0.011s^{-1}$-$0.17s^{-1}$), with a considerable variation from one subject to another. This is better illustrated for three selected samples in Fig. 5, where the apparent rate constants $f_{app}^{\max}$ and $g_{app}^{\max}$ are shown as a function of time for GB 1, 9 and 37 for both variable and constant value of $g_{app}^{\max}$. The peak active stresses of GB 1, 9 and 37 are 19mmHg, 70mmHg and 38mmHg, respectively. Physiologically, it seems reasonable to speculate that $f_{app}^{\max}$ would reflect the change of active stress, i.e. both $f_{app}^{\max}$ and $g_{app}^{\max}$ may be subject-dependent.

The variation of $\Delta\left[Ca^{2+}\right]$ estimated from (19) for subjects 1, 9 and 37 during the time of active muscle contraction is shown in Fig. 6. Note that the subject 9 the largest intracellular $\Delta\left[Ca^{2+}\right]$ (27.7nM/L), whereas the subject 1 has the smallest $\Delta\left[Ca^{2+}\right]$ (7.6nM/L). $\Delta\left[Ca^{2+}\right]$ for subject 37 is 13.78nM/L.

We can now correlate the parameters of the smooth muscle contraction to the GB pain induced by CCK test. These parameters are the peak f_{app}, the peak active stress, and the peak $[Ca^{2+}]$. However, the difficulty here is that there is no literature data on the threshold of pain using any of these constants. Hence we have extracted the "threshold" from the model that corresponds to the measured total stress threshold at which pain occurs (Li et al. 2011). This gives $[f_{app}]=0.051s^{-1}$, $[\sigma_a]=60$mmHg, and $[Ca^{2+}]=23$nM/L. The results are listed in Table 2. The success rates, defined as the positive correlation (e.g. $f_{app} > [f_{app}]$) over the total sample size, are 0.667 for the rate of attachment, active stress, $[Ca^{2+}]$ concentration, respectively. Overall, the correlation of these parameters is lower than using the total stress (which has over 76% success rate) (Li et al. 2011). As the total stress is the sum of the active

and passive stresses, this suggests that the pain receptors are associated with physical stretching and not the chemical stimulus alone.

5 Discussion

In this paper, we presented a model to extract the cross-bridge information of human GB smooth muscle from the routine clinical ultrasound scans. By using the Huxley's two-state cross-bridge model and the active stresses estimated from a simple mechanical model, we estimated the rate of constants of the cross-bridge models, as well as the increased Ca^{2+} concentration of the smooth muscle of GB walls. These results were achieved without directly measuring the concentrations of Mp+AMp in the smooth muscle cells, which is not attainable from routine clinical diagnoses. Thus our mode may provide a simple and non-invasive way of estimating possible smooth muscle malfunction, and an additional clinical assessment tool.

Our model is based on the cross-bridge models proposed by (Hai and Murphy 1988a). However, recent work suggests that there may be a cooperative interaction among the contractile proteins in rabbit portal vein smooth muscle. The phosphorylation of myosin light chain causes activation of unphosphorylated myosin (Vyas et al. 1992), causing dephosphorylated myosin to attach to actin to maintain the force. Such a cooperative activation of myosin contributes to a high tension with low levels of MLCP, and represents a different model to the one we used. However, we have not exploited the differences of using the cooperative interaction model since it has been reported that the new model did not show significant difference from those of the original four-state cross-bridge (Rembold and Murphy 1993; Rembold et al. 2004).

It is believed that normally smooth muscle contraction is based on the thick (myosin)-filament regulator mechanism, while the vertebrate striated muscles contraction is initiated by thin(actin)-filament control, where regulatory proteins (troponin & tropomyosin) limit the cross-bridge cycling until Ca^{2+} binds to troponin (Somlyo et al. 1988). However, in the absence of Ca^{2+}, vertebrate smooth muscle contraction appears to be thin-filament regulated and cooperative (Somlyo et al. 1988; Haeberle 1999), which is achieved by the PKC pathway (Morgan and Gangopadhyay 2001). It has been tested that for GB smooth muscle stimulated by a high CCK dose the pathway is thick-filament regulation. At a low dose CCK, because the thin-filament PKC pathway is very sensitive to low Ca^{2+} concentration, it adopts thin-filament mechanism (Yu et al. 1994; Yu et al. 1998).

More recently, Hai and Kim (2005) proposed a new model which can incorporate the thin-filament-based regulation (Hai and Kim 2005), as an extension to their previous four-state cross-bridge with an ultra-slow latch-bridge cycle (Hai and Murphy 1988a). The new model can achieve a steadily growing isometric active stress with decreasing MLCP concentration against time as shown the *in vitro* experiments for the airway smooth muscle stimulated by 1μM phorbol dibutyrate (PDBu), which is a specific stimulant for PKC pathway. Thus this more recent model seems to be able to deal with both thick-filament and thin-filament regulatory mechanisms. However, we choose not to use this model here as our premier interest is to investigate patients given a high dose of CCK in the CCK provocation tests. Caution is required in defining the "high dose CCK" here, as we performed CCK injection of 0.05 $\mu g / kg$ to patients, which is not directly convertible to the high dose (10^{-2} mM/L) used in laboratories. However, we can estimating the CCK concentration based on the estimated volume of blood contained per kilogram in men and women and the dose of CCK-10 that was given suggests that the likely concentrations are similar to the high dose by (Yu et al. 1994).

The apparent rate constants f_{app}^{max} and g_{app}^{max} in Table 1 stand for the averaged behaviour of single cross-bridge in smooth muscle (Lecarpentier et al. 2002). They are sensitive to species-and type of smooth muscles, presumably because of variable myosin concentration or degree of phosphorylation of myosin required in the smooth muscle cells. The apparent rate constants estimated in the paper appear to support this observation, although more experiments will be needed for acquisition of data.

However, in the current work, we have made the following assumptions: (1) that the GB remains as an ellipsoid during emptying and refilling, although the shape change is reflected by the axes ratio change; (2) that the pressure in the GB is constant during refilling; and (3) that the apparent rate constant g_{app} is estimated from the guinea pig data, and (4) that the r is used to represent the total number of binding per cross-bridge for just one site at actin per myosin head, while more recent studies suggest that it is likely that there may exist more than ten sites of actin binding per myosin head for smooth muscles (Rembold et al. 2004).

In addition, we have only estimated the apparent attachment rate constant in the isometric contraction of human GBs only. In other words, we only considered the smooth muscle contraction at the beginning of emptying. This may not be sufficient to identify other GB motility issues (or gallstone formation) associated with the whole emptying process.

Among these assumptions, perhaps the greatest limitation is the first one, since we know GB is attached to liver, which will put 3D constraint during its contraction. While this issue should be addressed with more sophisticated stress modelling, this will not change the qualitative results that are presented here. The estimation of the calcium concentration in the current model may be validated when experimental data become available. For example, it was confirmed experimentally that the apparent rate constant g_{app} of skinned rabbit adductor magnus fibres is Ca^{2+} concentration dependent during isometric contraction (Kerrick et al. 1991). For smooth muscles, however, such dependence is yet to be observed.

5 Conclusions

In this paper, we use a combination of cross-bridge and mechanical models for estimation of the parameters of a two-state cross-bridge model and the increased intracellular Ca^{2+} concentration from active stress computed for human GB data from clinical ultrasound scans. These parameters are obtained for 51 patients who underwent CCK provocation tests. The model supports the positive correlation between these parameters and the CCK induced GB pain, in the same manner as the correlation between the active stress and GB pain. However, the correlation is not as strong as that of the total (active + passive) stress, suggesting that pain receptors may be associated with physical stretching and not with smooth muscle contraction alone. The model also suggests that the rate of constants may be subject-dependent. Such an investigation linking the macro-scale mechanics to the micro-scale structure of smooth muscles of GB is useful for the in-depth understanding of human GB motility, and may pave a way for effective diagnoses and drug treatment.

Acknowledgements

The project was supported by EPSRC through the grants of EP/G015651 and EP/G028257.

References

Beuckelmann, D., M. Nabauer, et al. (1992). "Intracellular calcium handling in isolated ventricular myocytes from patients with terminal heart failure." Circulation **85**(3): 1046.

Brenner, B. (1988). "Effect of Ca2+ on cross-bridge turnover kinetics in skinned single rabbit psoas fibers: implications for regulation of muscle contraction." Proceedings of the National Academy of Sciences of the United States of America **85**(9): 3265.

Brotschi, E., K. Crocker, et al. (1989). "Effect of low extracellular calcium on gallbladder contractionin vitro." Digestive diseases and sciences **34**(3): 360-366.

Bursztyn, L., O. Eytan, et al. (2007). "Mathematical model of excitation-contraction in a uterine smooth muscle cell." American Journal of Physiology- Cell Physiology **292**(5): C1816.

Cozzolino, H., F. Goldstein, et al. (1963). "The cystic duct syndrome." JAMA **185**(12): 920.

Gwathmey, J. and R. Hajjar (1990). "Relation between steady-state force and intracellular [Ca2+] in intact human myocardium. Index of myofibrillar responsiveness to Ca2+." Circulation **82**(4): 1266.

Haeberle, J. (1999). "Thin-filament linked regulation of smooth muscle myosin." Journal of Muscle Research and Cell Motility **20**(4): 363-370.

Hai, C. M. (1991). "Length-dependent myosin phosphorylation and contraction of arterial smooth muscle." Pflügers Archiv European Journal of Physiology **418**(6): 564-571.

Hai, C. M. and H. R. Kim (2005). "An expanded latch-bridge model of protein kinase C-mediated smooth muscle contraction." Journal of Applied Physiology **98**(4): 1356.

Hai, C. M. and R. A. Murphy (1988a). "Cross-bridge phosphorylation and regulation of latch state in smooth muscle." American Journal of Physiology- Cell Physiology **254**(1): 99-106.

Hai, C. M. and R. A. Murphy (1988b). "Regulation of shortening velocity by cross-bridge phosphorylation in smooth muscle." American Journal of Physiology- Cell Physiology **255**(1): C86.

Hai, C. M. and R. A. Murphy (1989). "Cross-bridge dephosphorylation and relaxation of vascular smooth muscle." American Journal of Physiology- Cell Physiology **256**(2): C282.

Huxley, A. (1957). "Muscle structure and theories of contraction." Progress in biophysics and biophysical chemistry **7**: 255.

Ishizuka, J., M. Murakami, et al. (1993). "Age-related changes in gallbladder contractility and cytoplasmic Ca2+ concentration in the guinea pig." American Journal of Physiology-Gastrointestinal and Liver Physiology **264**(4): 624-629.

Kamm, K. and J. Stull (1985a). "The function of myosin and myosin light chain kinase phosphorylation in smooth muscle." Annual Review of Pharmacology and Toxicology **25**(1): 593-620.

Kamm, K. and J. Stull (1985b). "Myosin phosphorylation, force, and maximal shortening velocity in neurally stimulated tracheal smooth muscle." American Journal of Physiology- Cell Physiology **249**(3): C238.

Kerrick, W., J. Potter, et al. (1991). "The apparent rate constant for the dissociation of force generating myosin crossbridges from actin decreases during Ca 2+ activation of skinned muscle fibres." Journal of Muscle Research and Cell Motility **12**(1): 53-60.

Kroon, M. (2009). "A constitutive model for smooth muscle including active tone and passive viscoelastic behaviour." Mathematical Medicine and Biology.

Lecarpentier, Y., F. Blanc, et al. (2002). "Myosin cross-bridge kinetics in airway smooth muscle: a comparative study of humans, rats, and rabbits." American Journal of Physiology- Lung Cellular and Molecular Physiology **282**(1): L83.

Lee, K., P. Biancani, et al. (1989). "Calcium sources utilized by cholecystokinin and acetylcholine in the cat gallbladder muscle." American Journal of Physiology-Gastrointestinal and Liver Physiology **256**(4): 785.

Li, W., X. Luo, et al. (2011). "A Mechanical Model for CCK-Induced Acalculous Gallbladder Pain." Annals of biomedical engineering **39**(2): 786-800.
Li, W., X. Luo, et al. (2008). "Correlation of mechanical factors and gallbladder pain." Computational and Mathematical Methods in Medicine **9**(1): 27.
Mbikou, P., A. Fajmut, et al. (2011). "Contribution of Rho kinase to the early phase of the calcium–contraction coupling in airway smooth muscle." Experimental Physiology **96**(2): 240.
Meiss, R. (1975). "Graded activation in rabbit mesotubarium smooth muscle." American Journal of Physiology **229**(2): 455.
Morgan, K. and S. Gangopadhyay (2001). "Signal Transduction in Smooth Muscle: Invited Review: Cross-bridge regulation by thin filament-associated proteins." Journal of Applied Physiology **91**(2): 953.
Murtada, S. I., M. Kroon, et al. (2010). "A calcium-driven mechanochemical model for prediction of force generation in smooth muscle." Biomechanics and modeling in mechanobiology: 1-14.
Ratz, P., C. Hai, et al. (1989). "Dependence of stress on cross-bridge phosphorylation in vascular smooth muscle." American Journal of Physiology- Cell Physiology **256**(1): C96.
Rembold, C. and R. Murphy (1993). "Models of the mechanism for crossbridge attachment in smooth muscle." Journal of Muscle Research and Cell Motility **14**(3): 325-334.
Rembold, C., R. Wardle, et al. (2004). "Cooperative attachment of cross bridges predicts regulation of smooth muscle force by myosin phosphorylation." American Journal of Physiology- Cell Physiology **287**(3): C594.
Renzetti, L. M., M. B. Wang, et al. (1990). "Contribution of intracellular calcium to gallbladder smooth muscle contraction." American Journal of Physiology-Gastrointestinal and Liver Physiology **259**(1): 1-5.
Robertson, S., J. Johnson, et al. (1981). "The time-course of Ca2+ exchange with calmodulin, troponin, parvalbumin, and myosin in response to transient increases in Ca2+." Biophysical journal **34**(3): 559-569.
Shaffer, E., A. Bomzon, et al. (1992). "The source of calcium for CCK-induced contraction of the guinea-pig gall bladder." Regulatory peptides **37**(1): 15-26.
Shen, P., B. Fang, et al. (2007). "Effect of traditional Chinese herbs for nourishing the liver on intracellular free calcium level in gallbladder cells of guinea pigs with gallstones." Zhong xi yi jie he xue bao= Journal of Chinese integrative medicine **5**(2): 179.
Si, X., L. Huang, et al. (2009). "Inhibitory effects of somatostatin on cholecystokinin octapeptide induced bile regurgitation under stress: Ionic and molecular mechanisms." Regulatory peptides **156**(1-3): 34-41.
Singer, H. and R. Murphy (1987). "Maximal rates of activation in electrically stimulated swine carotid media." Circulation Research **60**(3): 438.
Smythe, A., R. Ahmed, et al. (2004). "Bethanechol provocation testing does not predict symptom relief after cholecystectomy for acalculous biliary pain." Digestive and Liver Disease **36**(10): 682-686.
Smythe, A., A. Majeed, et al. (1998). "A requiem for the cholecystokinin provocation test?" Gut **43**(4): 571.
Solaro, R. and H. Rarick (1998). "Troponin and tropomyosin: proteins that switch on and tune in the activity of cardiac myofilaments." Circulation Research **83**(5): 471.
Somlyo, A., Y. Goldman, et al. (1988). "Cross-bridge kinetics, cooperativity, and negatively strained cross-bridges in vertebrate smooth muscle. A laser-flash photolysis study." The Journal of general physiology **91**(2): 165.

Stålhand, J., A. Klarbring, et al. (2008). "Smooth muscle contraction: mechanochemical formulation for homogeneous finite strains." Progress in biophysics and molecular biology **96**(1-3): 465-481.

Thompson, M., A. Kliewer, et al. (2000). "Increased cardiomyocyte intracellular calcium during endotoxin-induced cardiac dysfunction in guinea pigs." Pediatric Research **47**(5): 669.

Vyas, T., S. Mooers, et al. (1992). "Cooperative activation of myosin by light chain phosphorylation in permeabilized smooth muscle." American Journal of Physiology-Cell Physiology **263**(1): C210.

Washabau, R. J., M. B. Wang, et al. (1994). "Role of myosin light-chain phosphorylation in guinea pig gallbladder smooth muscle contraction." American Journal of Physiology-Gastrointestinal and Liver Physiology **266**(3): 469-474.

Williamson, R. (1988). "Acalculous disease of the gall bladder." Gut **29**(6): 860.

Yang, J., J. W. Clark, et al. (2003a). "The myogenic response in isolated rat cerebrovascular arteries: smooth muscle cell model." Medical Engineering and Physics **25**(8): 691-709.

Yang, J., J. W. Clark, et al. (2003b). "The myogenic response in isolated rat cerebrovascular arteries: vessel model." Medical Engineering and Physics **25**(8): 711-717.

Yu, P., Q. Chen, et al. (1998). "Signal transduction pathways mediating CCK-induced gallbladder muscle contraction." American Journal of Physiology- Gastrointestinal and Liver Physiology **275**(2): 203.

Yu, P., G. De Petris, et al. (1994). "Cholecystokinin-coupled intracellular signaling in human gallbladder muscle." Gastroenterology **106**(3): 763.

Yu, S., P. Crago, et al. (1997). "A nonisometric kinetic model for smooth muscle." American Journal of Physiology- Cell Physiology **272**(3): C1025.

Zhang, W., C. Chung, et al. (2006). "Derivation and left ventricular pressure phase plane based validation of a time dependent isometric crossbridge attachment model." Cardiovascular Engineering **6**(4): 132-144.

Zulliger, M., A. Rachev, et al. (2004). "A constitutive formulation of arterial mechanics including vascular smooth muscle tone." American Journal of Physiology- Heart and Circulatory Physiology **287**(3): H1335.

Figure
Click here to download Figure: paperII-figure-06-Sept-2011-xyl.pdf

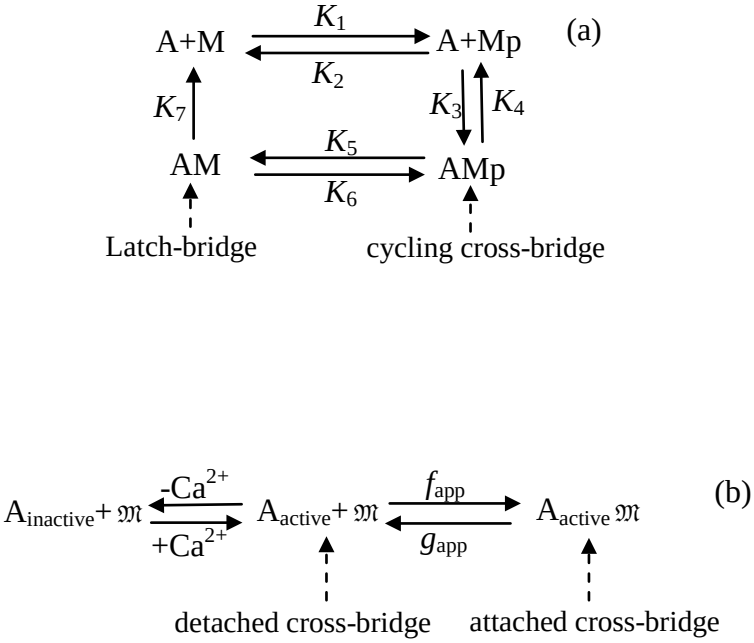

Fig. 1 (a) Structure of four-state thick filament-regulated latch cross-bridge model: K_1 to K_7 are rate constants, A denotes actin (thin fileaments), M detached dephosphorylated cross-bridge, Mp detached phosphorylated cross-bridges (i.e. latch-bridges). (b) Structure of the equivalent two-state model: f_{app} and g_{app} are the apparent rate constants for attachment and detachment, respectively; A_{active} and $A_{inactive}$ denote actin (thin filament) in absence and presence of Ca^{2+}, respectively; $\mathfrak{M}$, cross-bridges.

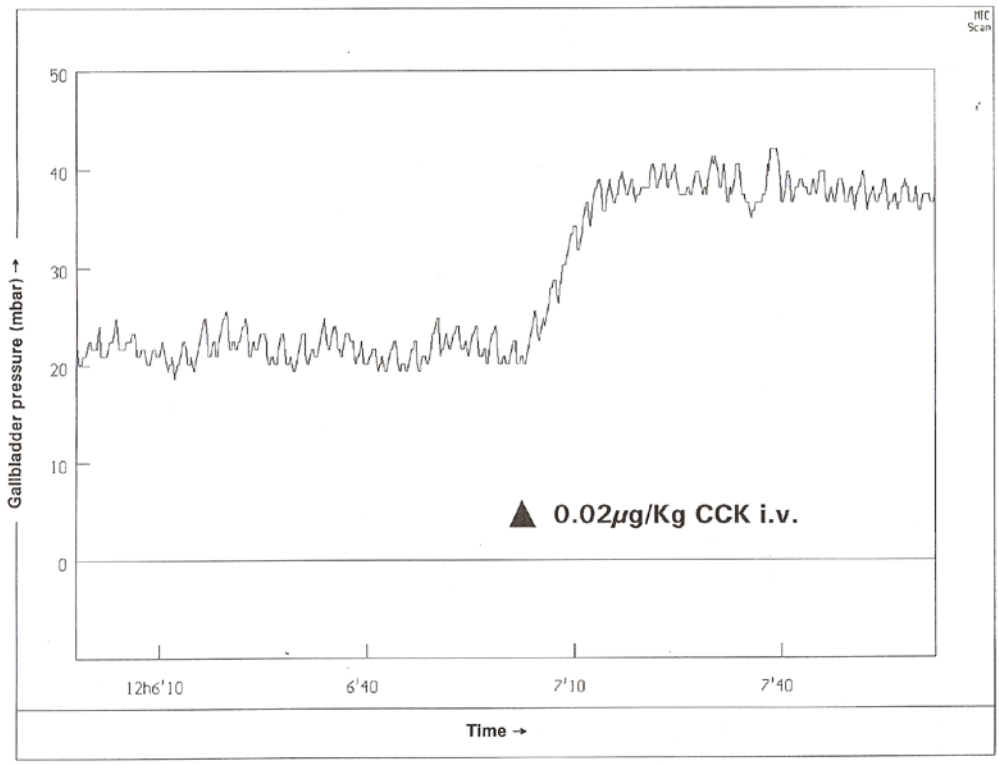

Fig. 2 Typical in vivo pressure measurement inside a GB against time before and after a certain CCK stimulant is applied. The pressure reaches a steady higher pressure after about 14 seconds from the basal pressure.

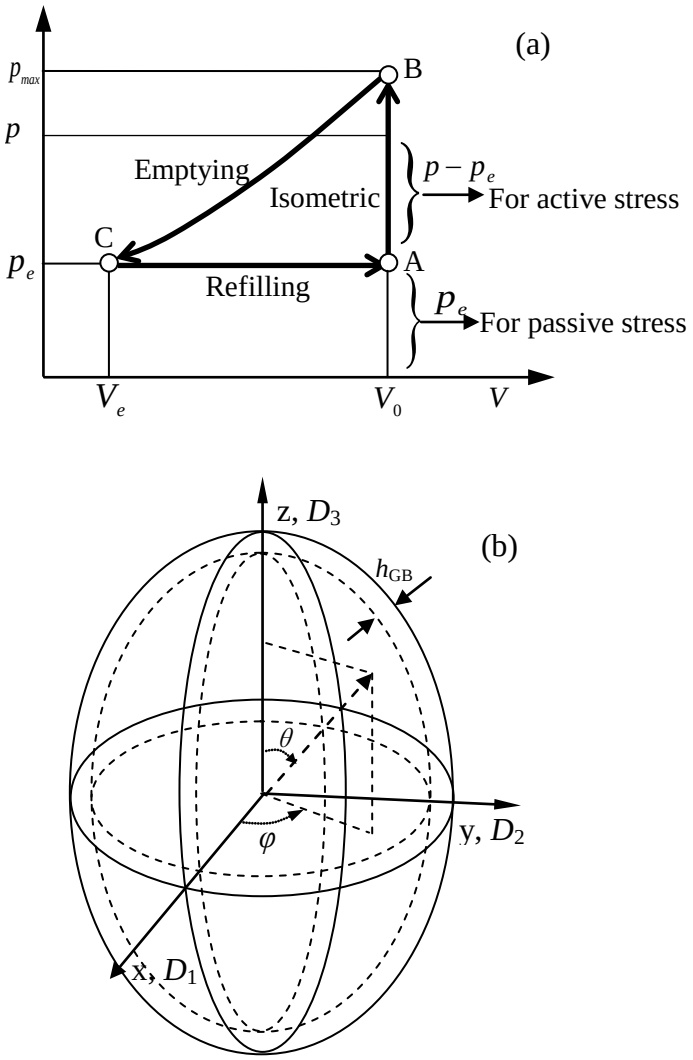

Fig. 3 *p-V* diagram (a) during refilling, isometric contraction and emptying phases in CCK provocation test, and ellipsoid GB model (b)

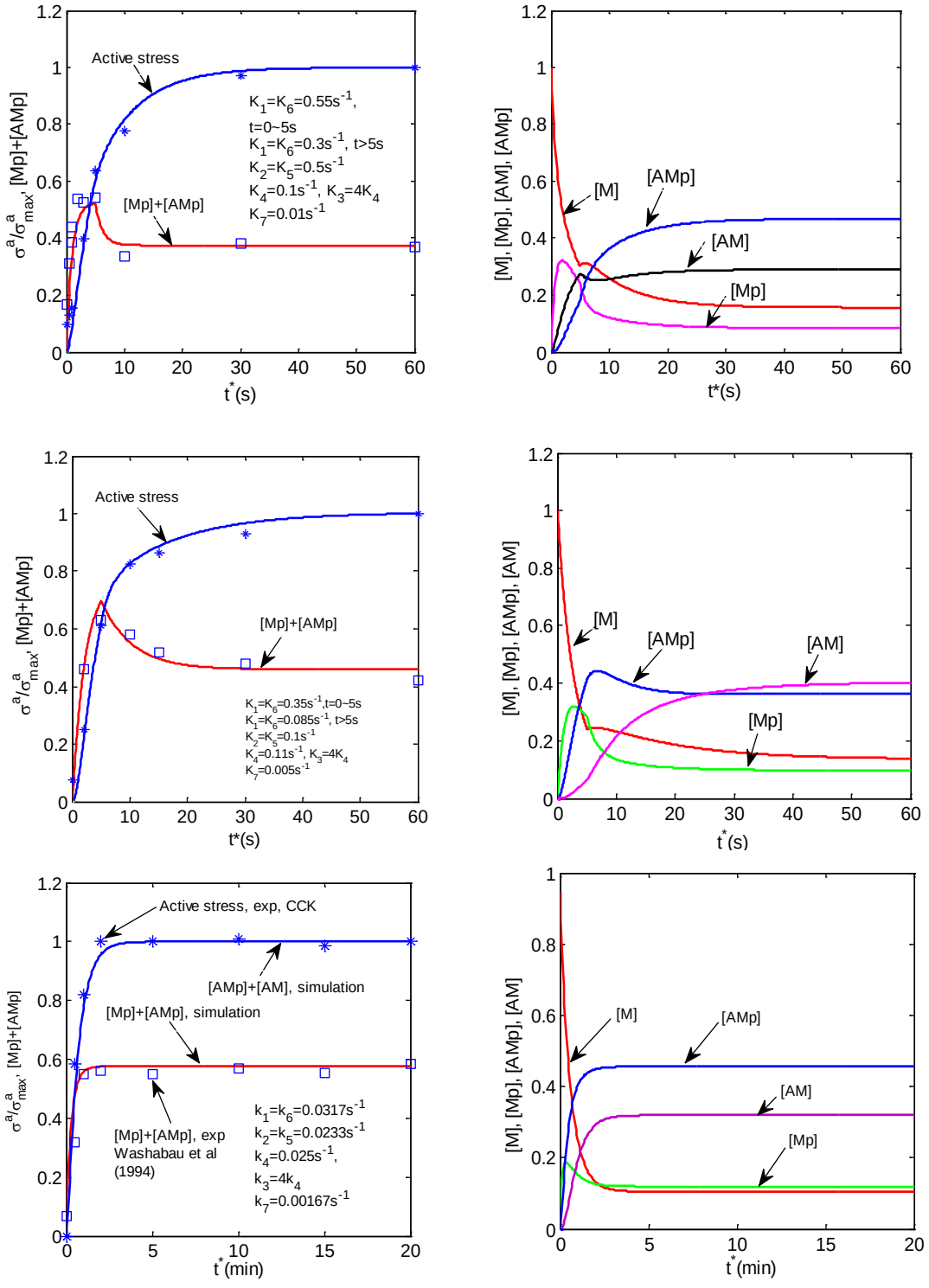

(a) (b)

Fig. 4 The dimensionless active stress (column a), and concentration (column b), plotted as functions of time. The top row is for the stimulated swine carotid artery smooth muscle (Singer and Murphy 1987). The middle row is for the tracheal smooth muscle (Kamm and Stull 1985b), and the bottom raw is for a guinea pig gallbladder smooth muscle (Washabau, Wang et al. 1994). The symbols represent the experimental data and curves denote the results predicted by the four-state cross-bridges model.

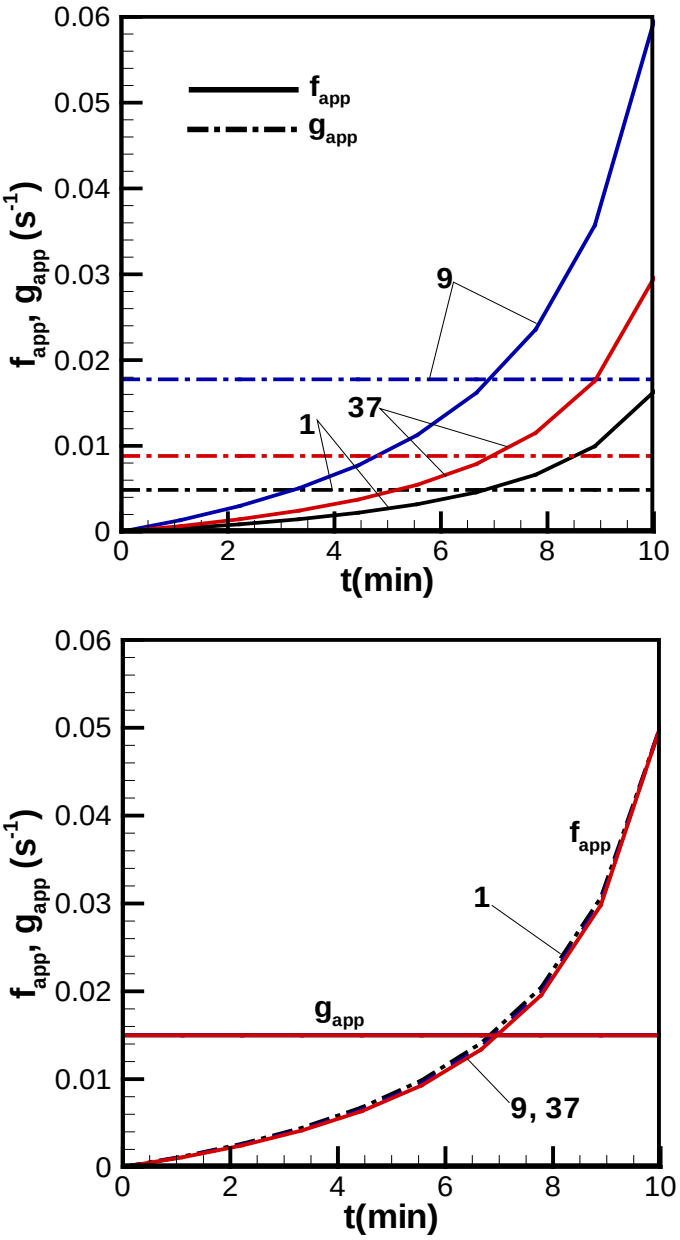

Fig. 5 The attachment and detachment apparent rate constants f_{app} (solid) and g_{app} (dashed) for gallbladder 1, 9 and 37 versus time, for (a) variable g_{app}, and (b) constant g_{app}. In both cases, r_{max} =0.77.

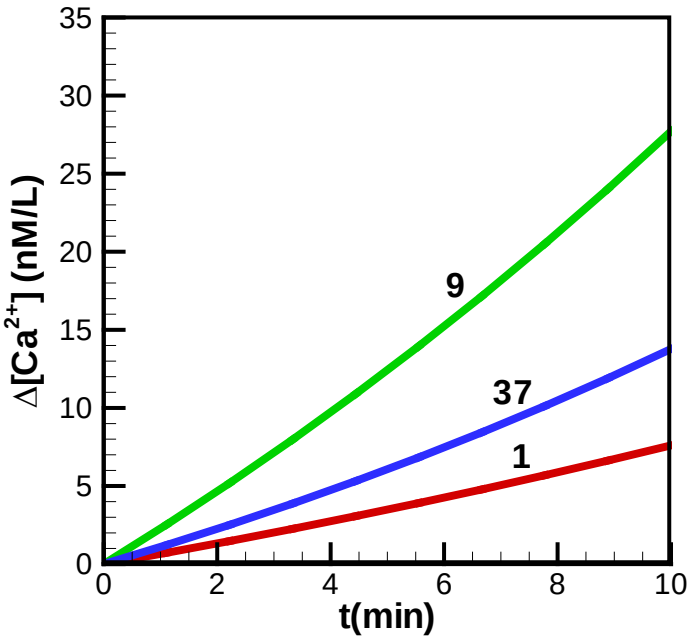

Fig. 6 The increased [Ca^{2+}] as function of time for the subject 1, 9 and 37, respectively.

Table 1 The maximum values of the apparent rate constants $f_{app}^{\max}$ and $g_{app}^{\max}$ estimated using the 4-state cross-bridge model for three different types of smooth muscles.

Smooth muscle	$f_{app}^{\max}$ (s^{-1})	$g_{app}^{\max}$ (s^{-1})
Swine carotid	0.2032	0.0575
Bovine tracheal	0.3455	0.1021
Guinea pig gallbladder	0.0553	0.0154

Table 2 Peak active stress, apparent rate constant and increased [Ca^{2+}] concentration of 51 patients

	EF(%)	λ (min^{-1})	Peak active stress (mmHg)	Variable g_{app}		Constant g_{app}		$\Delta[Ca^{2+}]$ (nM/L)	CCK Test
				Peak f_{app} (s^{-1})	Peak g_{app} (s^{-1})	Peak f_{app} (s^{-1})	Peak g_{app} (s^{-1})		
1	4.5	0.0327	19	0.0163	0.0049	0.050	0.015	7.47	no pain
2	5.4	0.0570	56	0.0329	0.0141	0.050	0.015	22.02	no pain
3	11.4	0.0498	37	0.0312	0.0093	0.050	0.015	14.55	no pain
4	15.5	0.0619	55	0.0469	0.0140	0.050	0.015	21.63	no pain
5	10.7	0.0270	48	0.0406	0.0121	0.050	0.015	18.87	pain(+)
6	10.0	0.0399	67(+)	0.0572(+)	0.0171	0.050	0.015	26.35(+)	pain(+)
7	14.0	0.0429	46	0.0390	0.0116	0.050	0.015	18.09	no pain
8	21.9	0.0577	90(+)	0.0763(+)	0.0228	0.050	0.015	35.39(+)	pain(+)
9	16.1	0.0418	70(+)	0.0595(+)	0.0178	0.050	0.015	27.53(+)	pain(+)
10	5.4	0.0398	96(+)	0.0814(+)	0.0243	0.050	0.015	37.75(+)	no pain
11	15.1	0.0613	152(+)	0.1295(+)	0.0387	0.050	0.015	59.77(+)	no pain
12	21.3	0.0413	56	0.0477	0.0142	0.050	0.015	22.02	no pain
13	39.7	0.0384	62(+)	0.0526(+)	0.0157	0.050	0.015	24.38(+)	pain(+)
14	20.6	0.0406	96(+)	0.0817(+)	0.0244	0.050	0.015	37.75(+)	pain(+)
15	80.8	0.0515	61(+)	0.0523(+)	0.0156	0.050	0.015	23.99(+)	pain(+)
16	32.3	0.0258	13	0.0114	0.0034	0.050	0.015	5.11	no pain
17	32.4	0.0409	27	0.0227	0.0068	0.050	0.015	10.61	pain(+)
18	93.7	0.0370	22	0.0189	0.0056	0.050	0.015	8.65	pain(+)
19	49.4	0.0873	102(+)	0.0865(+)	0.0258	0.050	0.015	40.11(+)	pain(+)
20	48.7	0.0446	32	0.0271	0.0081	0.050	0.015	12.58	pain(+)
21	66.3	0.0572	47	0.0403	0.0120	0.050	0.015	18.48	no pain
22	54.4	0.0312	20	0.0166	0.0050	0.050	0.015	7.86	pain(+)
23	44.7	0.0582	126(+)	0.1073(+)	0.0321	0.050	0.015	49.55(+)	pain(+)
24	27.4	0.0507	61(+)	0.0518(+)	0.0155	0.050	0.015	23.99(+)	no pain
25	27.9	0.0690	120(+)	0.1021(+)	0.0305	0.050	0.015	47.17(+)	pain(+)
26	19.1	0.0531	84(+)	0.0716(+)	0.0214	0.050	0.015	33.03(+)	pain(+)

27	70.2	0.0429	32	0.0273	0.0081	0.050	0.015	12.58	pain(+)
28	71.5	0.0477	35	0.0298	0.0089	0.050	0.015	13.76	no pain
29	37.8	0.0442	31	0.0262	0.0078	0.050	0.015	12.19	no pain
30	91.8	0.0483	68(+)	0.0581(+)	0.0173	0.050	0.015	26.739(+)	pain(+)
31	100	0.0408	98(+)	0.0831(+)	0.0248	0.050	0.015	38.54(+)	pain(+)
32	10.1	0.0413	56	0.0477	0.0142	0.050	0.015	22.02	no pain
33	95.0	0.0470	42	0.0359	0.0107	0.050	0.015	16.52	no pain
34	28.4	0.0367	83(+)	0.0704(+)	0.0210	0.050	0.015	32.64(+)	pain(+)
35	100	0.0209	19	0.0166	0.0050	0.050	0.015	7.47	pain(+)
36	16.3	0.0440	50	0.0429	0.0128	0.050	0.015	19.66	no pain
37	26.3	0.0477	38	0.0296	0.0088	0.050	0.015	13.78	no pain
38	10.7	0.0543	76(+)	0.0648(+)	0.0194	0.050	0.015	29.88(+)	pain(+)
39	8.0	0.0549	43	0.0371	0.0111	0.050	0.015	16.91	pain(+)
40	22.2	0.0298	24	0.0191	0.0057	0.050	0.015	9.44	pain(+)
41	36.4	0.0386	35	0.0204	0.0061	0.050	0.015	13.76	pain(+)
42	2.8	0.0888	107(+)	0.0911(+)	0.0272	0.050	0.015	42.07(+)	no pain
43	14.2	0.0554	201(+)	0.171(+)	0.0512	0.050	0.015	79.04(+)	pain(+)
44	15.2	0.0378	70(+)	0.0597(+)	0.0178	0.050	0.015	27.53(+)	no pain
45	9.1	0.0377	30	0.0255	0.0076	0.050	0.015	11.80	no pain
46	6.5	0.0472	40	0.0344	0.0103	0.050	0.015	15.73	no pain
47	0.34	0.0439	59	0.0502	0.0150	0.050	0.015	23.20	no Pain
48	0.08	0.0442	80(+)	0.0678(+)	0.0203	0.050	0.015	31.46(+)	Pain(+)
49	1.25	0.0252	40	0.0345	0.0103	0.050	0.015	15.73	Pain(+)
50	8.75	0.0657	85(+)	0.0524(+)	0.0157	0.050	0.015	33.42(+)	no pain
51	1.62	0.0403	64(+)	0.0542(+)	0.0162	0.050	0.015	25.17(+)	Pain(+)
Success rate			34/51=0.667	34/51=0.667				34/51=0.667	